Sparse Diagonal Forms for Translation Operators for the Helmholtz Equation in Two Dimensions

Vladimir Rokhlin

Research Report YALEU/DCS/RR-1095
December 27, 1995

YALE UNIVERSITY
DEPARTMENT OF COMPUTER SCIENCE

In the design of Fast Multipole Methods (FMM) for the numerical solution of scattering problems, a crucial step is the diagonalization of translation operators for the Helmholtz equation. These operators have analytically simple, physically transparent, and numerically stable diagonal forms. It has been observed by several researchers that for any given precision ε, diagonal forms for the translation operators for the Helmholtz equation are not unique, and that some choices lead to more efficient FMM schemes than others. As is well-known, original single-stage FMM algorithms for the Helmholtz equation have asymptotic CPU time requirements of order $O(n^{3/2})$, where n is the number of nodes in the discretization of the boundary of the scatterer; two-stage versions have CPU time estimates of order $O(n^{4/3})$; generally, $k-$stage versions have CPU time estimates of order $O(n^{(k+2)/(k+1)})$. However, there exist choices of diagonal forms leading to single-stage FMM algorithms with CPU time requirements of order $O(n^{4/3})$, two-stage schemes with CPU time requirements $O(n^{5/4})$, etc. In this paper, we construct such diagonal forms in two dimensions. While the construction of this paper is in no sense optimal, it is rigorous and straightforward. Our numerical experiments indicate that it is within a factor of two of being optimal, in terms of the number of nodes required to discretize the translation operator to a specified precision ε. The procedure is illustrated with several numerical examples.

Sparse Diagonal Forms for Translation Operators for the Helmholtz Equation in Two Dimensions

Vladimir Rokhlin
Research Report YALEU/DCS/RR-1095
December 27, 1995

This work was supported in part by ONR grant N00014-89-J-1527, and by ARPA grant F49620-93-1-0575.
Approved for public release: distribution is unlimited.
Keywords: *Fast Algorithms, Fast Multipole Method, Helmholtz Equation, Scattering Problems*

Sparse Diagonal Forms for Translation Operators for the Helmholtz Equation in Two Dimensions

1 Introduction

In the design of Fast Multipole Methods (FMM) for the numerical solution of scattering problems, a crucial step is the diagonalization of translation operators for the Helmholtz equation. These operators have analytically simple, physically transparent, and numerically stable diagonal forms. Once the latter are constructed, the design of FMM schemes is straightforward; the simplest "single-stage" algorithms have CPU time requirements of order $O(n^{3/2})$, where n is the number of nodes in the discretization of the problem. Two-stage schemes have CPU time requirements of order $O(n^{4/3})$; generally, $k-$stage schemes have CPU time requirements of order $O(n^{(k+2)/(k+1)})$.

It has been observed by several researchers (see, for example, [4, 2, 3]) that for any given precision ε, diagonal forms for the translation operators for the Helmholtz equation are not unique, and that some choices lead to more efficient FMM schemes than others. In fact, there exist choices of diagonal forms leading to single-stage FMM algorithms with CPU time requirements of order $O(n^{4/3})$, two-stage schemes with CPU time requirements $O(n^{5/4})$, etc.

Due to space limitations, we will not describe here the FMM for the Helmholtz equation, referring the reader to [6], [7]. We will observe that the functions $b^{\rho}_{r,\varepsilon} : [0, 2\pi] \rightarrow \mathbf{C}$ defined below are a generalization of functions $\nu_n : [0, 2\pi] \rightarrow \mathbf{C}$ of [6]. However, while the functions ν_n (see (3.25) in [6]) are nowhere small on the interval $[0, 2\pi]$, the functions $b^{\rho}_{r,\varepsilon}$ are negligibly small on most of their interval of definition. The cost of this sparsity is a somewhat higher frequency content of the functions $b^{\rho}_{r,\varepsilon}$; both the functions ν_n, $b^{\rho}_{r,\varepsilon}$ are trigonometric polynomials of finite order, and the order of $b^{\rho}_{r,\varepsilon}$ is 1.5 times higher than the order of ν_n under similar conditions. The result of this trade-off is a reduction in the cost of the algorithm (see the preceding two paragraphs). For a more detailed motivation for the development of improved translation operators for the Helmholtz equation, we refer the reader to the papers [4, 2, 3].

The purpose of this paper is to construct such diagonal forms in two dimensions. The construction is intended to be reasonably rigorous; it is also quite simple. However, the proof that the resulting translation operator is sparse is quite long and somewhat technical. Thus, discussion is deliberately conducted on two levels. First, we formulate the problem (Subsection 1.1), and describe **a** solution (Subsection 1.2). The solution of Subsection 1.2 has been chosen for analytical simplicity, rather than for its numerical properties. A more numerically attractive solution is described in Subsection 5.1 and illustrated in Subsection 5.1 by numerical examples. Thus, a reader who is not interested in the proofs may want to read Subsections 1.1, 1.2, and turn to Subsections 5.2, 5.2, possibly after reading Subsection 1.3 (informal description of the construction).

Otherwise, the structure of the paper is as follows. In Section 2, we summarize the known facts from analysis to be used in the remainder of the paper. In Section 3, we develop the

requisite analytical apparatus. In Section 4, we prove that the functions $b^{\rho}_{r,\varepsilon}$ introduced in this section do in fact satisfy the conditions 1. - 3. of this section. Finally, Section 5 contains a slightly modified construction of the functions $b^{\rho}_{r,\varepsilon}$ (quite similar to that of this section, but leading to somewhat faster computations), illustrated by several numerical examples.

Remark 1.1 The mathematical techniques used in this paper are limited to elementary analysis; however, the constructions we use are fairly involved. Thus, the proof of the principal analytical result of this paper (Theorem 1.1) consists of a fairly long sequence of definitions and lemmas. Most of the latter follow immediately from the preceding ones and from the relevant definitions, and in such cases the proofs are omitted.

1.1 Statement of the problem

In agreement with standard practice, we will denote by J_m the Bessel function of the first kind of order m, by H_m the Hankel function of order m, and by I_m the modified Bessel function of order m (see, for example, [1], Chapter 9).

Suppose that r, ρ, ε are three real numbers, such that

$$0 < 4 \cdot r < \rho, \tag{1}$$

and

$$0 < \varepsilon < 1/10. \tag{2}$$

We will denote by ν the smallest of all positive integer numbers such that

$$J_j(r) < \varepsilon. \tag{3}$$

for all $j > \nu$. The purpose of this paper is to construct a function $b^{\rho}_{r,\varepsilon} : [0, 2\pi] \to \mathbb{C}$, satisfying the following conditions.

1. There exist a positive integer λ (independent of ρ and r, but possibly dependent on ε) and complex $\alpha_{-\lambda\cdot\nu}, \alpha_{-\lambda\cdot\nu+1}, \alpha_{-\lambda\cdot\nu+2}, \cdots, \alpha_{-1}, \alpha_0, \alpha_1, \cdots, \alpha_{\lambda\cdot\nu-1}, \alpha_{\lambda\cdot\nu}$, such that

$$b^{\rho}_{r,\varepsilon}(\theta) = \sum_{j=-\lambda\cdot\nu}^{\lambda\cdot\nu} \alpha_j \cdot e^{i\cdot j\cdot\theta}, \tag{4}$$

for all $\theta \in [-\pi, \pi]$.

2. For all $j \in [-2\cdot\nu, 2\cdot\nu]$,

$$| \alpha_j - H_k(\rho) | < \varepsilon. \tag{5}$$

3. There exist two numbers p, q, independent of r and ρ (though possibly dependent on ε), such that

$$| b^{\rho}_{r,\varepsilon}(\theta) | < \varepsilon \tag{6}$$

for all $\theta \in [-\pi, \pi]$ such that

$$| \theta | > \frac{p}{r} + q \cdot \frac{r}{\rho}. \tag{7}$$

Remark 1.2 From the point of view of asymptotic CPU time estimates, it is sufficient to construct functions $b^{\rho}_{r,\varepsilon}$ satisfying the conditions 1. - 3. above. In terms of actual computation times, it is critical that the coefficients λ, p, q be as small as possible. In the construction of the following subsection, $\lambda = 3$; Theorem 1.1 formulated in the following subsection (to be proved in Section 4) provides values $p = 8 \cdot \sqrt{2} \cdot log(1/\varepsilon)$, $q = 8$. The actual values are considerably smaller, as can be seen from the numerical examples presented in Section 5.

Remark 1.3 In this paper we construct several solutions of the Helmholtz equation that are negligibly small over most of the complex plane, without being equal to zero. We will also be dealing with restrictions of such solutions on circles and lines in the plane. Abusing the terminology somewhat, when we say that the support of some function is contained by some region, we mean that outside that region, the absolute value of the function is smaller than a preselected ε.

1.2 Construction of the functions $b^{\rho}_{r,\varepsilon}$

In this subsection, we construct functions $b^{\rho}_{r,\varepsilon}$ satisfying the conditions 1. - 3. of Subsection 1.1.

We will denote by μ the smallest integer such that

$$\mu > (r^{\frac{1}{3}} + c \cdot r^{-\frac{1}{3}})^3, \tag{8}$$

with

$$c = \frac{3^{-1/3}}{2} \cdot \delta^{\frac{2}{3}}, \tag{9}$$

$$\delta = log(\frac{1}{\varepsilon}), \tag{10}$$

and by u the real number defined by the formula

$$u = \frac{r^2}{8 \cdot \delta}. \tag{11}$$

We will define two positive integer numbers m, n via the formulae

$$m = 6 \cdot \mu \tag{12}$$

$$n = \frac{5}{2} \cdot \mu, \tag{13}$$

respectively, and by $f_{\varepsilon,r}$ the function $[-\pi, \pi] \rightarrow \mathbf{C}$, defined by the formula

$$f_{\varepsilon,r}(\theta) = \frac{sin((n + \frac{1}{2}) \cdot \theta)}{sin(\frac{\theta}{2})} \cdot e^{u \cdot (cos(\theta) - 1)}. \tag{14}$$

Finally, for each $\rho > 4 \cdot r$, we will define the function $b^{\rho}_{r,\varepsilon} : [-\pi, \pi] \to \mathbf{C}$ by the formula

$$b^{\rho}_{r,\varepsilon}(\theta) = \sum_{j=-m/2}^{m/2} (\widehat{f_{\varepsilon,r}})_j \cdot H_j(\rho) \cdot e^{i \cdot j \cdot \theta}, \tag{15}$$

where $(\widehat{f_{\varepsilon,r}})_j$ denotes the $j-th$ Fourier coefficient of the function $f_{\varepsilon,r} : [-\pi, \pi] \to \mathbf{C}$.

The following theorem states that the function $b^{\rho}_{r,\varepsilon}$ satisfies the conditions 1. - 3. of the preceding subsection, and provides estimates for the coefficients p, q in (7). Its proof is the principal purpose of Sections 3, 4 of this paper.

Theorem 1.1 *Suppose that r, ρ, ε are three real numbers satisfying the inequalities (1), (2), and the function $b^{\rho}_{r,\varepsilon}$ is defined by (15). Then*

1. For all $j \in [-2 \cdot \nu, 2 \cdot \nu]$,

$$| (\widehat{b^{\rho}_{r,\varepsilon}})_j - H_k(\rho) | < \varepsilon. \tag{16}$$

2.

$$| b^{\rho}_{r,\varepsilon}(\theta) | < \varepsilon \tag{17}$$

for all $\theta \in [-\pi, \pi]$ such that

$$| \theta | > \frac{8 \cdot \sqrt{2} \cdot log(\frac{1}{\varepsilon})}{r} + 8 \cdot \frac{r}{\rho}. \tag{18}$$

1.3 Outline of the proof of Theorem 1.1

Put informally, Theorem 1.1 states that given real numbers r, ρ such that $4 \cdot r < \rho$, there exists a function $b : [-\pi, \pi] \to \mathbf{C}$ such that

a. b is a trigonometric polynomial of order m, with $m \sim 3 \cdot r$.

b. The first $4 \cdot r$ coefficients in the Fourier series of b are defined by the formula

$$(\hat{b})_j = H_j(\rho) \tag{19}$$

for all j such that $| j | < 2 \cdot r$.

c. $b(\theta)$ is small for all θ outside a small neighborhood of the point $\theta = 0$. More specifically, the size of the region around 0 where $b(\theta) > \varepsilon$ may depend on ε, but has to be of the order r/ρ.

In this formulation, it is clear that Theorem 1.1 is not at all obvious, except when $\rho \sim r^2$, or greater. Indeed, in this case,

$$H_m(z) \sim \sqrt{(\frac{2}{\pi \cdot r})} \cdot e^{i \cdot (z - \frac{m\pi}{2} \cdot \frac{\pi}{4})} \tag{20}$$

(see (39)), and the problem of finding a function satisfying the conditions a. - c. of this section becomes a classical problem of designing a low-pass filter that is (almost) band-limited in both time and frequency domains.

When ρ is considerably smaller than r^2 (which is normally the case in situations involving the FMM), such simple asymptotic techniques do not work. In this regime, Theorem 1.1 is a consequence of detailed analytical properties of Hankel functions, and its proof has to take these into account. In this paper, we observe that (4) can be rewritten as

$$b(\rho,\theta) = \sum_{j=-m/2}^{m/2} \gamma_j \cdot H_j(\rho) \cdot e^{i\cdot j\cdot\theta}, \tag{21}$$

with the condition (5) assuming the form

$$|\,\gamma_j - 1\,| < \varepsilon. \tag{22}$$

Now, we change our point of view, interpret the pair (ρ,θ) in (21) as polar coordinates of a point in R^2, and define the mapping $Q : \mathbf{R}^2 \to \mathbf{C}$ via the formula

$$Q(x,y) = b(\rho,\theta), \tag{23}$$

with (ρ,θ) the polar coordinates of the point $(x,y) \in \mathbf{R}^2$. Clearly, in this interpretation, Q is a solution of the Helmholtz equation (24) satisfying the radiation condition (27). Thus, the proof of Theorem 1.1 has been reduced to constructing a solution to the equation (24) possessing certain properties. Once such a solution is found, the function $b^{\rho}_{r,\varepsilon}(\theta)$ is obtained as a restriction of Q on the circle of radius ρ.

The conditions to be satisfied by Q follow immediately from the conditions a. - c. above. In addition to (22), Q must look like a beam to satisfy (17). Fortunately, beam-like solutions of the Helmholtz equation are well-known; a typical example are the so-called Gaussian beams (see Section 3 below). In this paper, we obtain functions (21) as linear combinations of Gaussian beams (see Section 4, where the resulting function $\mathbf{R}^2 \to \mathbf{C}$ is denoted by Q^n_u).

The last problem we encounter is the fact that Gaussian beams are not sufficiently sharp to satisfy the condition c. of Subsection 1.1; put differently, a Gaussian beam that is sufficiently sharp to satisfy the condition c. is singular on a region too large for the condition a. to be satisfied. Fortunately, Gaussian beams can be modified to reduce the size of the singular region dramatically, leaving the beam almost intact away from the singularity. Section 3 is largely devoted to this construction, which is referred to as Modified Gaussian Beam.

2 Analytical Preliminaries

In this section, we summarize several facts from analysis to be used in the sections below. All of these facts are either well-known, or follow immediately from well-known facts.

2.1 Notation.

For the Helmholtz equation

$$\nabla^2\phi + k^2\phi = 0 \tag{24}$$

we will define the potential $\phi^k_{x_0} : \mathbf{R}^2 \setminus \{x_0\} \to \mathbf{C}$ of a unit charge located at the point $x_0 \in \mathbf{R}^2$ by the formula

$$\phi^k_{x_0}(x) = H_0(k\|x - x_0\|), \tag{25}$$

where H_0 denotes the Hankel function of order zero. We will define the potential $\phi^k_{x_0,h}$ of a unity dipole located at x_0 and oriented in the direction $h \in \mathbf{R}^2$ by the formula

$$\phi^k_{x_0,h}(x) = -H_1(k\|x - x_0\|) \cdot \frac{k(x - x_0, h)}{\|x - x_0\|}, \tag{26}$$

where H_1 denotes the Hankel function of order one. In most cases, a potential ϕ satisfying the equation (24) in an unbounded region, also satisfies the radiation condition at ∞, i.e. for any $x \in \mathbf{R}^2$, there exists $c \in \mathbf{C}$ such that

$$\lim_{t \to \infty} \psi(t \cdot x) \cdot e^{-ikt \cdot |x|} \cdot \sqrt{t} = c, \tag{27}$$

and will refer to functions satisfying the equation (24) (and in unbounded regions - also the condition (27)) as radiation potentials.

Remark 2.1 In the remainder of the paper, we will be assuming that the Helmholtz coefficient k in (24) - (27) equal to 1, unless explicitly stated otherwise.

For an arbitrary set $D \in \mathbf{R}^2$ and a point $x \in \mathbf{R}^2$, we will denote by $T_x(D)$ the set of all points y in $\mathbf{R}^2$ such that $y - x \in D$.

Given a set $D \subset \mathbf{R}^2$ and a positive real number r, we will denote by $S_r(D)$ the set of all points $x \in \mathbf{R}^2$ such that $x = x_0 + y$, with $x_0 \in D$, and y some vector in $\mathbf{R}^2$ such that $\|y\| \leq r$. The following obvious lemma provides a bound on the radius of $S_r(D)$ given the radius of D.

Lemma 2.1 *Suppose that D is a subset of $\mathbf{R}^2$, and $\rho > 0$ is a real number, such that $\|x_0\| \leq \rho$ for all $x_0 \in D$. Then $\|x\| \leq r + \rho$ for any $x \in S_r(D)$*

In Subsection 2.2, we will need the following lemma; its proof is an exercise in elementary calculus, and is omitted.

Lemma 2.2 *For any positive real x, t and natural k,*

$$\frac{e^{\frac{x}{2} \cdot (1 + \frac{k}{x} + \frac{x}{x+k})}}{(1 + \frac{k}{x})^k} \leq e^x \cdot e^{-\frac{k^2}{2 \cdot x}} \cdot e^{\frac{k^4}{6 \cdot x^3}}. \tag{28}$$

2.2 Elementary properties of Bessel functions

As is well-known, there exist two functions $\alpha, \beta : \mathbf{C} \to \mathbf{C}$, such that

$$H_0(z) = \alpha(z) + \beta(z) \cdot log(z) \tag{29}$$

for all $z \in C$; the functions H_0, H_1 are connected by the formula

$$H_1(z) = -\frac{d}{dz} H_0(z). \tag{30}$$

The following lemma provides a crude (but sufficient for our purposes) estimate of the absolute values of the Hankel functions H_0, H_1. It is an immediate consequence of 9.1.12, 9.1.13, 9.2.1, 9.2.7 in [1].

Lemma 2.3 *For any $z \in C$,*

$$| H_0(z) | < \frac{e^{-Im(z)}}{\sqrt{|z|}}, \tag{31}$$

and

$$| H_1(z) | < e^{-Im(z)} \cdot (\frac{1}{\sqrt{|z|}} + \frac{1}{|z|}). \tag{32}$$

As is well known (see, for example, [8]), J_m are analytic on the whole complex plane for all integer values of m, while H_m have a branch cut along the negative real axis, and become infinite at the origin. The asymptotic behavior of the functions J_m, H_m for large m is given by the formulae

$$\lim_{m \to \infty} J_m(z) \cdot (\frac{2m}{ez})^m \cdot \sqrt{(2\pi m)} = 1, \tag{33}$$

$$\lim_{m \to \infty} H_m(z) \cdot (\frac{ez}{2m})^m \cdot \frac{\sqrt{(\pi m)}}{\sqrt{2}} = -1 \tag{34}$$

(see [1], 9.3.1, 9.3.2, 9.1.3). It is immediately clear from (33) that the functions $J_m(z)$ decay rapidly when z is fixed and m is large. However, (33) is an asymptotic statement, understating the actual rate of decay of (33) when m is only slightly greater than $| z |$. For purely imaginary z, a dramatically stronger estimate is given by Lemma 2.7 below; for purely real z, a fairly tight estimate is provided by the following lemma, which can be found in [8], pp. 227, 255.

Lemma 2.4 *For any real $0 < x < 1$ and $\nu > 0$,*

$$J_\nu(\nu \cdot x) < \frac{x^\nu \cdot e^{\nu \cdot \sqrt{(1-x^2)}}}{(2 \cdot \pi \cdot \nu)^{\frac{1}{2}} \cdot (1-x^2)^{\frac{1}{4}} \cdot (1 + \sqrt{(1-x^2)})^\nu}. \tag{35}$$

The following lemma provides a simplified version of (35). Given (35), its proof is an exercise in elementary calculus, and is omitted.

Lemma 2.5 *For any real* $r > 10$ *and* $0 < \varepsilon < 0.1$,

$$J_n(r) < \varepsilon \tag{36}$$

for any

$$n > (r^{\frac{1}{3}} + c \cdot r^{-\frac{1}{3}})^3, \tag{37}$$

with c, δ *defined by (9), (10).*

Remark 2.2 Obviously, if n satisfies the inequality (37) and ν is defined by (3), then $\nu < n$.

For large z and fixed m, the asymptotic behavior of $J_m(z)$, $H_m(z)$ is given by the formulae

$$\sqrt{z}J_m(z) - \sqrt{(\frac{2}{\pi})}\cos(z - \frac{m\pi}{2} - \frac{\pi}{4}) = O(\frac{e^{Im(z)}}{|z|}), \tag{38}$$

$$\sqrt{z}H_m(z) - \sqrt{(\frac{2}{\pi})}e^{i(z - \frac{m\pi}{2} - \frac{\pi}{4})} = O(\frac{e^{-Im(z)}}{|z|}) \tag{39}$$

when $z \rightarrow \infty$, as long as $Im(z) \geq 0$ (see [1], 9.2.5, 9.2.7).

We will need the behavior of Bessel functions in one more asymptotic regime, as provided by the following lemma, which can be found (in a slightly different form) in [8].

Lemma 2.6 *For any integer* $n > 0$,

$$\frac{1}{2} \cdot \frac{\Gamma(\frac{1}{3})}{2^{2/3} \cdot 3^{1/3} \cdot \pi \cdot n^{1/3}} < J_n(n) < \frac{\Gamma(\frac{1}{3})}{2^{2/3} \cdot 3^{1/3} \cdot \pi \cdot n^{1/3}} \cdot 2. \tag{40}$$

Furthermore,

$$\lim_{n \rightarrow \infty} \frac{2^{2/3} \cdot 3^{1/3} \cdot \pi \cdot n^{1/3}}{\Gamma(\frac{1}{3})} \cdot J_n(n) = 1. \tag{41}$$

As is well-known, the modified Bessel functions I_m are defined by the formula

$$I_m(z) = i^{-n} \cdot J_m(i \cdot z) \tag{42}$$

for all complex z; we will need the classical formula

$$e^{\frac{z}{2} \cdot (t + \frac{1}{t})} = \sum_{k=-\infty}^{\infty} t^k \cdot I_k(z), \tag{43}$$

valid for all pairs z, t such that $t \neq 0$.

It is well-known that once $n > z$, the functions $J_n(z)$ decay rapidly with n (see (33), (35)), for all complex z. What appears to be less well-known, is that when z is purely imaginary, the decay starts at $n \sim \sqrt{(2 \cdot z)}$. The following lemma provides a somewhat crude description of the behavior of $I_n(x)$ in the regime $\sqrt{(2 \cdot x)} < n < x$. We present an outline of the proof for this lemma, since the author has failed to find it in the literature.

Lemma 2.7 *For any integer n and real x such that $0 \leq n \leq x$,*

$$I_n(x) \leq e^x \cdot e^{-\frac{n^2}{2 \cdot x}} \cdot e^{\frac{n^4}{6 \cdot x^3}}. \tag{44}$$

Proof.

Since $I_k(x) > 0$ for all positive k, x, it immediately follows from (43) that

$$I_k(x) \leq \frac{e^{\frac{x}{2} \cdot (t + \frac{1}{t})}}{t^k} \tag{45}$$

for all positive real t, x and natural k. In particular, (45) holds for $t = 1 + \frac{k}{x}$, becoming

$$I_k(x) \leq \frac{e^{\frac{x}{2} \cdot (1 + \frac{k}{x} + \frac{x}{x+k})}}{(1 + \frac{k}{x})^k}. \tag{46}$$

Now, (44) follows from Lemma 2.2 above.

□

The following technical lemma is obtained from the preceding one by elementary algebraic manipulation.

Lemma 2.8 *Suppose that r, u, δ are three positive real numbers, and n is an integer number. Suppose further that δ, c, u are defined by (10), (9), (11), respectively, and n satisfies the inequality (37). Then*

$$I_n(u) \leq e^u \cdot e^{-\delta}. \tag{47}$$

Finally, we will need two well-known integral expressions for Bessel functions, given by the following lemma.

Lemma 2.9 *For any integer n and complex z,*

$$J_n(z) = \frac{i^{-n}}{2 \cdot \pi} \cdot \int_0^{2\pi} e^{i \cdot z \cdot cos(\theta)} \cdot e^{i \cdot n \cdot \theta} d\theta, \tag{48}$$

and

$$I_n(z) = \frac{1}{2 \cdot \pi} \cdot \int_0^{2\pi} e^{z \cdot cos(\theta)} \cdot e^{i \cdot n \cdot \theta} d\theta. \tag{49}$$

2.3 Green's formula for the Helmholtz equation

The following theorem is a special case of the famous Green's formula. It can be found (for example) in [5].

Theorem 2.10 *Suppose that the function $\phi : \mathbf{R}^2 \to \mathbf{C}$ satisfies the Helmholtz equation (24) outside the region Ω with boundary Γ. Suppose further that it satisfies the outgoing radiation condition (26) at ∞. Than for any $x \in \mathbf{R}^2 \setminus \bar{\Omega}$,*

$$\phi(x) = -\frac{i}{4} \cdot \int_\Gamma (\phi(t) \cdot \frac{\partial G}{\partial N}(t,x) + \frac{\partial \phi}{\partial N}(t) \cdot G(t,x)) dl, \tag{50}$$

with

$$G(x,y) = H_0(k \cdot ||x-y||) \tag{51}$$

for any $x, y \in \mathbf{R}^2$ such that $x \neq y$; the integration in (50) is with respect to the arc length.

2.4 Partial wave expansions of radiation potentials

Suppose that a function $\psi : \mathbf{R}^2 \to \mathbf{C}$ satisfies the Helmholtz equation (24) outside the disk D of radius R with the center at the point $x_0 \in \mathbf{R}^2$, and that it also satisfies the radiation condition (26) at ∞. Then there exists a unique sequence $\alpha = \{\alpha_m\}, m = 0, 1, 2, \cdots$, such that for any $x \in \mathbf{R}^2 \setminus \bar{D}$,

$$\psi(x) = \sum_{m=-\infty}^{+\infty} \alpha_m \cdot H_m(k\rho) \cdot e^{im\theta}. \tag{52}$$

In the above formula, $\rho = ||x - x_0||$ and θ is the angle between the vector $x - x_0$ and the x axis.

A derivation of the formula (52) can be found, for example, in [5]; we will refer to expansions of the form (52) as H-expansions, and to the point x_0 as the center of the expansion (52).

The following lemma is a direct consequence of the formulae (33), (34). It establishes the convergence rate of the expansion (52).

Lemma 2.11 *If $D_2 \subset D$ is a disk of radius $R_2 > R$ with the center at x_0 then there exists $c > 0$ such that for any $x \in \mathbf{R}^2 \setminus \bar{R}_2$ and $N > |k| \cdot R$,*

$$|\psi(x) - \sum_{m=-N}^{N} \beta_m \cdot H_m(k\rho) \cdot e^{im\theta}| < c \cdot (\frac{R}{R_2})^N. \tag{53}$$

Remark 2.3 In numerical calculations, the expansion (52) is truncated after a finite number of terms, and the resulting expression is viewed as an approximation to the potential ψ. As is well-known, if we want to approximate ψ by an expansion of the form (53) with accuracy ε, we have to choose

$$N \sim R \cdot | k |, \tag{54}$$

i.e. the number of terms in the approximation is almost independent of ε, and must be roughly equal to $|k| \cdot R$.

2.5 Far-field representations of radiation potentials

In this subsection, we introduce an alternative form of the expansion (52), possessing a simple physical interpretation simplifying many calculations with radiation potentials.

For the expansion (52), we will consider a function $F_{x_0}(\psi) : [-\pi, \pi] \to \mathbf{C}^1$ defined by the formula

$$F_{x_0}(\psi)(\theta) = \lim_{t \to \infty} \psi(t \cdot x + x_0) \cdot \sqrt{t} \cdot e^{-ikt} \cdot \frac{\sqrt{(k\pi)}}{\sqrt{2}} \cdot e^{\frac{\pi}{4} \cdot i} \tag{55}$$

with $x = (\cos\theta, \sin\theta)$. Substituting (39), (52) into (55), we immediately obtain

$$F_{x_0}(\psi)(\theta) = \sum_{m=-\infty}^{+\infty} \beta_m e^{-\frac{m\pi}{2} i} e^{im\theta}, \tag{56}$$

which provides an explicit expression for $F_{x_0}(\psi)$ via the coefficients $\{\beta_m\}$. Clearly, (56) defines a unitary mapping connecting the coefficients $\{\alpha_j\}$ in the expansion (52) with the with the function $F_{x_0}(\psi)$, and we will refer to $F_{x_0}(\psi)$ as the far-field representation of the radiation potential ψ with the origin at x_0.

Obviously, given a radiation potential (52), its far-field representation (55) depends on the origin x_0. The following lemma describes the dependence; its proof can be found (for example) in [6].

Lemma 2.12 *Suppose that the radiation potential ψ is defined by the formula (52), and x_0, x_1 are two arbitrary points in $\mathbf{R}^2$. Suppose further that $F_{x_0}(\psi)$, $F_{x_1}(\psi)$ are the far-field representations of ψ with origins x_0, x_1 respectively. Then for any $\theta \in [-\pi, \pi]$,*

$$F_{x_1}(\psi)(\theta) = F_{x_0}(\psi)(\theta) \cdot e^{i \cdot k \cdot ((x_1 - x_0), w)}, \tag{57}$$

with the vector $w \in \mathbf{R}^2$ defined by the formula

$$w = (cos(\theta), sin(\theta)). \tag{58}$$

Remark 2.4 In fact, both the existence of asymptotic representations of radiation fields and the above lemma are an immediate consequence of the radiation condition (27). A detailed investigation of such issues can be found in [6] in the two-dimensional case, and in [7] in the three-dimensional one.

The following lemma is an immediate consequence of the formulae (56), (52). It provides an explicit formula for the evaluation of a radiation potential at a point, given its far-field representation.

Lemma 2.13 *Suppose that a function $\psi : \mathbf{R}^2 \to \mathbf{C}$ satisfies the Helmholtz equation (24) outside the disk D of radius R with the center at the origin, and that ψ also satisfies the radiation*

condition (26) at ∞. Suppose further that $\sigma : [-\pi, \pi] \to \mathbf{C}$ is the far-field representation of ψ. Then for any $x \in \mathbf{R}^2 \setminus \bar{D}$,

$$\psi(x) = \sum_{m=-\infty}^{+\infty} (\hat{\sigma})_m \cdot e^{\frac{m\pi}{2}i} \cdot e^{im\theta} \cdot H_m(k \cdot \rho), \tag{59}$$

where (ρ, θ) are the polar coordinates of x, and $(\hat{\sigma})_m$ denotes the m-th term of the Fourier series of σ.

2.6 Gaussian Beams

Gaussian beams are solutions of the Helmholtz equation that are obtained as potentials of charges with complex coordinates. Such a potential is small everywhere outside a region in the plane that looks like a spreading beam, and inside that region the graph of the absolute value of such a function looks like the normal distribution; hence the term "Gaussian beam". Because of their localized nature, Gaussian beams are used as building blocks for the construction of other solutions for the Helmholtz equation.

Suppose that $u > 0$ is a real number. We will define the function $G_u : \mathbf{R}^2 \to \mathbf{C}$ by the formula

$$G_u(x, y) = H_0(\sqrt{((x - i \cdot u)^2 + y^2)}) \cdot e^{-u}, \tag{60}$$

and refer to G_u as a Gaussian beam with base u, oriented horizontally and pointing to the right. For any $x_0 \in \mathbf{R}^2$, we will denote by $G_u^{x_0}$ the mapping $\mathbf{R}^2 \to \mathbf{C}$, defined by the formula

$$G_u^{x_0}(x) = G_u(x + x_0). \tag{61}$$

Obviously, $G_u^0 = G_u$, and $G_u^{x_0}$ will also be referred to as a Gaussian Beam.

The following lemma provides an explicit expression for the far-field representation for the Gaussian beam (60). While its proof is very simple, we provide it, since it reveals important features of the behavior of Gaussian beams at large distances from the origin.

Lemma 2.14 *Suppose that u is a positive real number. Then the Gaussian beam (60) is a radiation potential outside the subset B_u of $\mathbf{R}^2$, consisting of all pairs (x, y) such that*

$$x = 0, \tag{62}$$

$$-u \leq y \leq u. \tag{63}$$

Furthermore, the far-field representation of (60) is given by the formula

$$F_0(G_u)(\theta) = e^{u \cdot (\cos(\theta) - 1)}, \tag{64}$$

for all $\theta \in [-\pi, \pi]$.

Proof. We start with observing that the equation

$$(x - i \cdot u)^2 + y^2 = 0 \tag{65}$$

has exactly two solutions:

$$(\quad x \quad = 0, \ y = -u), \tag{66}$$

$$(\quad x \quad = 0, \ \ y = u). \tag{67}$$

Thus, the function $G_u : \mathbf{R}^2 \to \mathbf{C}$ has logarithmic singularities at the points (66), (67), connected by a branch cut (see (29)); obviously, outside this branch cut the function (60) is analytic and satisfies the equation (24).

Suppose now that $x^2 + y^2 >> u^2$. Using the Taylor theorem, we have

$$\sqrt{((x - i \cdot u)^2 + y^2)} =$$

$$\sqrt{(x^2 + y^2)} \cdot \sqrt{(1 - \frac{2 \cdot i \cdot x \cdot u}{x^2 + y^2} - \frac{u^2}{x^2 + y^2})} =$$

$$\sqrt{(x^2 + y^2)} - i \cdot \frac{x \cdot u}{\sqrt{(x^2 + y^2)}} + O(\frac{1}{\sqrt{(x^2 + y^2)}}) =$$

$$r - i \cdot u \cdot cos(\theta) + O(\frac{1}{r}), \tag{68}$$

with (r, θ) the polar coordinates of the point $(x, y) \in \mathbf{R}^2$. Now, (64) follows from the combination of (68), (60), (55), (39).

□

Remark 2.5 An exercise in elementary calculus shows that for any $u > 0$,

$$e^{u \cdot (cos(\theta) - 1)} < -e^{-u \cdot \frac{\theta^2}{5}} \tag{69}$$

for all $\theta \in [-\pi, \pi]$, and

$$\max_{\theta \in [-\pi, \pi]} \mid e^{u \cdot (cos(\theta) - 1)} - e^{-u \cdot \frac{\theta^2}{2}} \mid < \frac{1}{u}, \tag{70}$$

Both bounds (70), (69) are quite crude, but sufficient for our purposes.

3 Detailed Analysis of Gaussian Beams

In this section, we develop the analytical apparatus to be used in Section 4 to prove Theorem 1.1. The principal tool we use consists of the well-known Gaussian beams; however, the analysis we use is somewhat more detailed than what appears to be present in the literature.

3.1 Four elementary lemmas

In this and the following subsections, we analyze the spatial structure of functions of the form (60) in some detail, in the process justifying the use of the term "Gaussian beams". Lemmas 3.1 - 3.4 below provide the necessary analysis. Their proofs are an exercise in elementary calculus, and are omitted. We start with several additional definitions.

For any positive real u, we will define the function $f : \mathbf{R}^2 \rightarrow \mathbf{C}$ by the formula

$$f(x,y) = \sqrt{((x - i \cdot u)^2 + y^2)}. \tag{71}$$

For any positive real u, β such that $\beta < u$, we will define two regions A, B in $\mathbf{R}^2$, as follows.

1. The region $A_{u,\beta}$ consists of all pairs (x,y), such that

$$| y | > \frac{\sqrt{((x^2 + \beta^2) \cdot (u^2 - \beta^2))}}{\beta}. \tag{72}$$

2. The region $B_{u,\beta}$ consists of all pairs (x,y), such that

$$| y | \leq \frac{\sqrt{((x^2 + \beta^2) \cdot (u^2 - \beta^2))}}{\beta} \tag{73}$$

(see Figure 1).

Lemma 3.1 *For any positive u, β such that $\beta < u$,*

$$R^2 = A_{u,\beta} \bigcup B_{u,\beta}. \tag{74}$$

Furthermore, for any $(x,y) \in A_{u,\beta}$,

$$Im(f(x,y)) < \beta, \tag{75}$$

and for any $(x,y) \in B_{u,\beta}$,

$$Im(f(x,y)) > \beta, \tag{76}$$

The preceding lemma describes precisely the part $A_{u,\beta}$, of the plane where the inequality (75) is satisfied; the following one provides a simplified approximate description of the region $A_{u,\beta}$.

Lemma 3.2 *Suppose that under the conditions of the preceding lemma, δ is a positive real number, such that*

$$\beta = u - \delta, \tag{77}$$

and

$$\delta + 1 < \frac{u}{2}. \tag{78}$$

Then

$$Im(f_u(x,y)) < u - \delta - 2 \cdot log(u) \tag{79}$$

for any $(x,y) \in R^2$ *such that*

$$| y | > 2 \cdot \sqrt{2} \cdot \sqrt{(\delta + 1) \cdot \frac{\sqrt{(x^2 + u^2)}}{\sqrt{u}}}. \tag{80}$$

The following lemma provides a further simplification of the conditions (72), (73) when $2 \cdot \sqrt{u} < \sqrt{(x^2 + y^2)} < 2 \cdot u$.

Lemma 3.3 *Suppose that the positive real numbers* x, u, δ *are such that*

$$\delta < \frac{u}{2}, \tag{81}$$

$$2 \cdot \sqrt{u} < x < 2 \cdot u \tag{82}$$

Then

$$Im(f_u(x,y)) < u - \delta \tag{83}$$

for any y *such that*

$$| y | > 2 \cdot \sqrt{(10 \cdot \delta) \cdot \sqrt{u}}. \tag{84}$$

Proof.

Obviously, (84), can be rewritten in the form

$$| y | > 2 \cdot \sqrt{(10 \cdot \delta) \cdot \sqrt{u}} = 2 \cdot \sqrt{(2 \cdot \delta) \cdot \frac{\sqrt{(4 \cdot u^2 + u^2)}}{\sqrt{u}}}. \tag{85}$$

Substituting (82) into (85), we obtain

$$| y | > 2 \cdot \sqrt{(2 \cdot \delta) \cdot \frac{\sqrt{(x^2 + u^2)}}{\sqrt{u}}}. \tag{86}$$

Now, (83) follows from the combination of (82) and Lemma 3.2.

□

The following lemma describes a simplification of the conditions (72), (73) when $\sqrt{(x^2 + y^2)} > 2 \cdot u$.

Lemma 3.4 *Suppose that the positive real numbers x, u, δ are such that*

$$\delta < \frac{u}{2}, \tag{87}$$

and

$$x \geq 2 \cdot u. \tag{88}$$

Then

$$Im(f_u(x,y)) < u - \delta \tag{89}$$

for any y such that

$$\frac{|\, y \,|}{x} > \frac{4 \cdot \sqrt{\delta}}{\sqrt{u}}. \tag{90}$$

Proof. Introducing the notation

$$\frac{x}{u} = \mu, \tag{91}$$

we observe that, due to (88), $\mu \geq 2$, and, therefore,

$$\frac{\sqrt{(1+\mu^2)}}{\mu} < \sqrt{2}. \tag{92}$$

Now, substituting (91) into (90), we have

$$\begin{aligned} &\frac{|\, y \,|}{x} > \frac{4 \cdot \sqrt{\delta}}{\sqrt{u}} > \frac{2 \cdot \sqrt{2} \cdot \sqrt{\delta} \cdot u \cdot \sqrt{(1+\mu^2)}}{\mu \cdot u^{3/2}} = \\ &\frac{2 \cdot \sqrt{2} \cdot \sqrt{\delta} \cdot u \cdot \sqrt{(u^2 + \mu^2 \cdot u^2)}}{\mu \cdot u^{3/2}} = \\ &\frac{2 \cdot \sqrt{2} \cdot \sqrt{\delta} \cdot u \cdot \sqrt{(u^2 + x^2)}}{\mu \cdot u^{3/2}}. \end{aligned} \tag{93}$$

Multiplying both sides of (93) by x and using (91) again, we get

$$\begin{aligned} &|\, y \,| > \frac{2 \cdot \sqrt{2} \cdot \sqrt{\delta} \cdot u \cdot \sqrt{(u^2 + \mu^2 \cdot u^2)}}{\mu \cdot u^{3/2}} \cdot x = \\ &\frac{2 \cdot \sqrt{2} \cdot \sqrt{\delta} \cdot \sqrt{(u^2 + x^2)}}{\sqrt{u}} \cdot x. \end{aligned} \tag{94}$$

Now, (89) follows from the combination of (94) and Lemma 3.2.

□

3.2 Geometry of Gaussian beams

In this subsection, we use the elementary lemmas of the preceding one to describe in some detail the spatial behavior of Gaussian beams. The theorem below follows immediately from the combination of Lemmas 3.3, 3.4 above and Lemma 2.3.

Theorem 3.5 *Suppose that the positive real numbers u, δ are such that*

$$\delta < \frac{u}{2}. \tag{95}$$

Then

$$| G_u(x,y) | < e^{-\delta} \tag{96}$$

in either of the following two (intersecting) regions:

1. $x \in [2 \cdot \sqrt{u}, 2 \cdot u]$, $| y | > 2 \cdot \sqrt{(10 \cdot \delta)} \cdot \sqrt{u}$.

2. $x \in [2 \cdot u, \infty]$, $| y | > \frac{4 \cdot \sqrt{\delta}}{\sqrt{u}} \cdot x$.

Observation 3.1 *The above theorem has a very transparent physical interpretation. Specifically, a Gaussian beam (60) begins to look like a beam once $x > \sqrt{u}$. While $x \in [\sqrt{u}, u]$, the Gaussian beam virtually does not expand. At approximately $x = u$, the beam begins to expand with the angle of expansion roughly $4 \cdot \sqrt{\delta}/\sqrt{u}$, with $e^{-\delta}$ relative error of our measurements (or calculations). This behavior is quite obvious in Figure 3.*

4 Modified and Modulated Gaussian Beams

4.1 Modified Gaussian beams

According to Lemma 2.14, the Gaussian beam (60) has a localized far-field representation. Specifically, for any $\varepsilon > 0$,

$$| F_0(G_u)(\theta) | < \varepsilon \tag{97}$$

for all θ such that

$$| \theta | > \sqrt{(\frac{5}{u} \cdot \log(\frac{1}{\varepsilon}))} \tag{98}$$

(see (69)). On the other hand, G_u has logarithmic singularities at the points (66), (67), and a branch cut connecting them. In other words, to a specified precision, the support of the far-field representation of a Gaussian beam is proportional to $1/\sqrt{u}$, with u the size of the region where the beam (60) is discontinuous. This very large region of discontinuity turns out to be a major problem when Gaussian beams are used as bricks for the construction of other solutions of the equation (24). Fortunately, there exist solutions of the equation (24) almost exactly coinciding with (60) away from the branch cut (62), (63), and singular on a region of

size roughly $\sqrt{u}$. We will refer to such solutions as Modified Gaussian Beams (MGBs), and use use them as building blocks for the construction of solutions of the equation (24). In this subsection, we construct the MGBs, and prove some of their properties. We start with several definitions.

For an arbitrary pair of positive real numbers u, δ, we will denote by R_1 the rectangle in the plane defined by the four vertices

$$(1, -(u+1)), (1, (u+1)), (-1, (u+1)), (-1, -(u+1)), \tag{99}$$

by R_4 the rectangle defined by its vertices

$$(2, -(u+2)), (2, (u+2)), (-2, -(u+2)), (-2, (u+2)), \tag{100}$$

by R_2 the rectangle defined by the vertices

$$(1, -\gamma), (1, \gamma), (-1, \gamma), (-1, -\gamma), \tag{101}$$

with

$$\gamma = 2 \cdot \sqrt{(2 \cdot u \cdot (\delta + 1))}, \tag{102}$$

and by R_3 the difference $R_1 \setminus R_2$, observing that R_3 consists of two rectangles, with vertices

$$(1, -\gamma), (1, -(u+1)), (-1, -(u+1)), (-1, -\gamma), \tag{103}$$

$$(1, \gamma), (1, (u+1)), (-1, (u+1)), (-1, \gamma), \tag{104}$$

respectively (see Figure 2). We will denote by Γ_1, Γ_2, Γ_3, Γ_4 the boundaries of the regions R_1, R_2, R_3, R_4, respectively. Whenever a function is to be integrated over one of these boundaries, the integration will always be assumed to be with respect to the arc length.

We will denote by $G_{u,\delta}$ the function $\mathbf{R}^2 \setminus R_2 \to \mathbf{C}$ defined by the formula

$$G_{u,\delta}(x) = -\frac{i}{4} \cdot \int_{\Gamma_2} (G_u(t) \cdot \frac{\partial G}{\partial N}(t, x) + \frac{\partial (G_u(t))}{\partial N}(t) \cdot G(t, x)) dl, \tag{105}$$

and refer to $G_{u,\delta}$ as a Modified Gaussian Beam. For any $x_0 \in \mathbf{R}^2$, we will denote by $G^{x_0}_{u,\delta}$ the mapping $T_{x_0}(\mathbf{R}^2 \setminus R_2) \to \mathbf{C}$, defined by the formula

$$G^{x_0}_{u,\delta}(x) = G_{u,\delta}(x + x_0). \tag{106}$$

Obviously, $G^0_{u,\delta} = G_{u,\delta}$, and $G^{x_0}_{u,\delta}$ will also be referred to as a Modified Gaussian Beam.

The following lemma shows that for large u, δ, the values $G_u(x)$ are almost zero for all $x \in \Gamma_3$. It is an immediate consequence of Lemma 3.2 and the formulae (103), (104).

Lemma 4.1 *Suppose that u, δ are two positive real numbers, such that $\delta < u/2$. Then for any $x \in \Gamma_3$,*

$$| G_u(x) | < \frac{e^{-\delta}}{u^2}. \tag{107}$$

The following lemma shows that for large u, δ, the functions $G_{u,\delta}$, G_u very nearly coincide for values of argument outside Γ_4.

Lemma 4.2 *Suppose that u, δ are two real positive numbers, such that $\delta + 1 < u/2$. Then for any $x \in \mathrm{R}^2 \setminus R_4$,*

$$| G_{u,\delta}(x) - G_u(x) | < e^{-\delta}. \tag{108}$$

Proof.

Since G_u is a solution of the equation (24), analytic outside R_1 and satisfying the radiation condition (26) at ∞, Theorem 2.1 yields

$$G_u(x) = -\frac{i}{4} \cdot \int_{\Gamma_1} (G_u(t) \cdot \frac{\partial G}{\partial N}(t,x) + \frac{\partial (G_u(t))}{\partial N}(t) \cdot G(t,x)) dl, \tag{109}$$

for any $x \in \mathrm{R}^2 \setminus \bar{R}_1$. Obviously (see Figure 2),

$$\begin{aligned} &\int_{\Gamma_1} (G_u(t) \cdot \frac{\partial G}{\partial N}(t,x) + \frac{\partial (G_u(t)}{\partial N}(t) \cdot G(t,x)) dl = \\ &\int_{\Gamma_2} (G_u(t) \cdot \frac{\partial G}{\partial N}(t,x) + \frac{\partial (G_u(t)}{\partial N}(t) \cdot G(t,x)) dl + \\ &\int_{\Gamma_3} (G_u(t) \cdot \frac{\partial G}{\partial N}(t,x) + \frac{\partial (G_u(t)}{\partial N}(t) \cdot G(t,x)) dl. \end{aligned} \tag{110}$$

On the other hand, it immediately follows from the combination of (31), (32), and (107) that

$$| \int_{\Gamma_3} (G_u(t) \cdot \frac{\partial G}{\partial N}(t,x) + \frac{\partial (G_u(t)}{\partial N}(t) \cdot G(t,x)) dl | < e^{-\delta}, \tag{111}$$

and we obtain (108) by combining (111) with (110) and (105).

□

The following lemma shows that the far-field representation of the modified Gaussian beam $G_{u,\delta}$ is almost identical to that of the Gaussian beam G_u. Its proof is similar to that of Lemma 4.2, and is omitted.

Lemma 4.3 *Suppose that u, δ are two real positive numbers, such that $\delta + 1 < u/2$. Then*

$$| F_0(G_{u,\delta})(\theta) - e^{u \cdot (\cos(\theta) - 1)} | < e^{-\delta}. \tag{112}$$

for all $\theta \in [-\pi, \pi]$.

4.2 Modulated Gaussian beams

We will define the function $M_u^m : \mathbf{R}^2 \to \mathbf{C}$ by the formula

$$M_u^n(x,y) = \frac{i^m}{J_m(m)} \cdot \sqrt{(\frac{i}{8 \cdot \pi})} \cdot \int_0^{2\pi} G_u(x - m \cdot cos(\eta), y - m \cdot sin(\eta)) \cdot e^{i \cdot m \cdot \eta} d\eta, \quad (113)$$

and the function $M_{u,\delta}^m : \mathbf{R}^2 \to \mathbf{C}$ by the formula

$$M_{u,\delta}^n(x,y) = \frac{i^m}{J_m(m)} \cdot \sqrt{(\frac{i}{8 \cdot \pi})} \cdot \int_0^{2\pi} G_{u,\delta}(x - m \cdot cos(\eta), y - m \cdot sin(\eta)) \cdot e^{i \cdot m \cdot \eta} d\eta \quad (114)$$

(the definitions (113), (114) are correct and stable due to Lemma 2.6). We will be referring to M_u^m as Modulated Gaussian Beam, and to $M_{u,\delta}^m$ as Modulated Modified Gaussian Beam (MMGB). Obviously, M_u^m is a radiation potential outside the region $S_m(B_u)$ (see (62), (63), and Lemma 2.1, and $M_{u,\delta}^m$ is a radiation potential outside $S_m(R_2)$ (see (101)). The following lemma supplies the far-field representation for M_u^m.

Lemma 4.4 *For any real $u > 0$ and integer m,*

$$F_0(M_u^m)(\theta) = e^{i \cdot m \cdot \theta} \cdot e^{u \cdot (cos(\theta) - 1)} \quad (115)$$

for all $\theta \in [-\pi, \pi]$.

Proof.

Combining (113) with (61) and (57), we have

$$F_0(M_u^m)(\theta) =$$
$$\frac{i^m}{J_m(m)} \cdot \sqrt{(\frac{i}{8 \cdot \pi})} \cdot \int_0^{2\pi} F_0(G_u^{(m \cdot cos(\eta), m \cdot sin(\eta))})(\theta) \cdot e^{i \cdot m \cdot \eta} d\eta =$$
$$\frac{i^m}{J_m(m)} \cdot \sqrt{(\frac{i}{8 \cdot \pi})} \cdot \int_0^{2\pi} F_{(m \cdot cos(\eta), m \cdot sin(\eta))}(G_u)(\theta) \cdot e^{i \cdot m \cdot \eta} d\eta =$$
$$\frac{i^m}{J_m(m)} \cdot \sqrt{(\frac{i}{8 \cdot \pi})} \cdot$$
$$F_0(G_u)(\theta) \cdot \int_0^{2\pi} e^{i \cdot k \cdot ((m \cdot cos(\eta), m \cdot sin(\eta)), (cos(\theta), sin(\theta)))} \cdot e^{i \cdot m \cdot \eta} d\eta =$$
$$\frac{i^m}{J_m(m)} \cdot \sqrt{(\frac{i}{8 \cdot \pi})} \cdot$$
$$F_0(G_u)(\theta) \cdot \int_0^{2\pi} e^{i \cdot k \cdot m \cdot (cos(\eta) \cdot cos(\theta) + sin(\eta) \cdot sin(\theta))} \cdot e^{i \cdot m \cdot \eta} d\eta =$$
$$\frac{i^m}{J_m(m)} \cdot \sqrt{(\frac{i}{8 \cdot \pi})} \cdot F_0(G_u)(\theta) \cdot \int_0^{2\pi} e^{i \cdot k \cdot m \cdot cos(\eta - \theta)} \cdot e^{i \cdot m \cdot \eta} d\eta. \quad (116)$$

Now, we obtain (115) by combining (116) with (48) and (64).

□

The following lemma is an immediate consequence of the combination of Lemmas 4.4, 4.3. It supplies the (approximate) far-field representation of $M^m_{u,\delta}$.

Lemma 4.5 *For any real $u > 0$, integer m, and $0 < \delta < u/2$,*

$$| F_0(M^m_{u,\delta})(\theta) - e^{i\cdot m\cdot\theta} \cdot e^{u\cdot(cos(\theta)-1)} | < e^{-\delta}, \tag{117}$$

for all $\theta \in [-\pi, \pi]$.

For an arbitrary integer $n > 0$, real $u > 0$, and real $0 < \delta < u/2$, we will define the function $Q^n_u : \mathbf{R}^2 \to \mathbf{C}$ via the formula

$$Q^n_u(x) = \sum_{m=-n}^{n} M^m_u(x), \tag{118}$$

and the function $Q^n_{u,\delta} : \mathbf{R}^2 \to \mathbf{C}$ via the formula

$$Q^n_{u,\delta}(x) = \sum_{m=-n}^{n} M^m_{u,\delta}(x). \tag{119}$$

Obviously, Q^n_u is a radiation potential outside $S_n(B_u)$ and $Q^n_{u,\delta}$ is a radiation potential outside $S_n(R_2)$.

The following two theorems describe the far-field representations of Q^n_u, $Q^n_{u,\delta}$, respectively. They follow immediately from Lemmas 4.4, 4.5, respectively, and the obvious fact that

$$\sum_{m=-n}^{n} e^{i\cdot m\cdot\theta} = \frac{sin((n+\frac{1}{2})\cdot\theta)}{sin(\frac{\theta}{2})}. \tag{120}$$

Theorem 4.6 *For an arbitrary integer $n > 0$ and real $u > 0$,*

$$F_0(Q^n_u)(\theta) = \frac{sin((n+\frac{1}{2})\cdot\theta)}{sin(\frac{\theta}{2})} \cdot e^{u\cdot(cos(\theta)-1)} \tag{121}$$

for all $\theta \in [-\pi, \pi]$.

Theorem 4.7 *For an arbitrary integer $n > 0$, real $u > 0$, and real $0 < \delta < u/2$,*

$$| F_0(Q^n_{u,\delta})(\theta) - \frac{sin((n+\frac{1}{2})\cdot\theta)}{sin(\frac{\theta}{2})} \cdot e^{u\cdot(cos(\theta)-1)} | < e^{-\delta} \tag{122}$$

for all $\theta \in [-\pi, \pi]$.

The following theorem is an immediate consequence of the combination of Theorem 3.5 with (119), (114), (108). It shows that the support of the function $Q^n_{u,\delta}$ is shaped like a beam, whose width is closely related to that of the Gaussian beam G_u.

Theorem 4.8 *Suppose that $n > 0$ is an integer number, and u, δ, are two real numbers such that $0 < \delta < u/2$. Then*

$$| Q^n_{u,\delta}(x,y) | < e^{-\delta} \tag{123}$$

in either of the following two (intersecting) regions:

1. $x \in [2 \cdot \sqrt{u}, 2 \cdot u]$, $| y | > 2 \cdot \sqrt{(10 \cdot \delta)} \cdot \sqrt{u} + n$.

2. $x \in [2 \cdot u, \infty]$, $| y | > \frac{4 \cdot \sqrt{\delta}}{\sqrt{u}} \cdot x + n$.

The following theorem is obtained from the preceding one by elementary algebraic manipulation.

Theorem 4.9 *Suppose that under the conditions of Theorem 4.8, the numbers u, n, are defined by (11), (13), respectively, and that in addition, $u > 2 \cdot \delta$. Then*

$$| Q^n_{u,\delta}(x,y) | < e^{-\delta} \tag{124}$$

in either of the following two (intersecting) regions:

1. $x \in [\frac{r}{\sqrt{2} \cdot \sqrt{\delta}}, \frac{r^2}{4 \cdot \delta}]$, $| y | > 8 \cdot r$.

2. $x \in [\frac{r^2}{4 \cdot \delta}, \infty]$, $| y | > 8 \cdot \sqrt{2} \cdot \delta \cdot \frac{x}{r}$.

Theorem 4.7 provides an analytical expression for the far-field representation $F_0(Q^n_{u,\delta})$ of the potential $Q^n_{u,\delta}$. The following theorem provides a somewhat less detailed description of the Fourier series of $F_0(Q^n_{u,\delta})$.

Theorem 4.10 *Suppose that under the conditions of Theorem 4.7, $r > 0$ is a real number, and the numbers u, δ, ν, n, m are defined by the formulae (11), (10), (3), (12), (13). Then for all integer j such that $| j | < 2 \cdot \nu$,*

$$| (F_0(\widehat{Q^n_{u,\delta}}))_j - 1 | < \varepsilon. \tag{125}$$

Furthermore, for any j such that $| j | > m/2$,

$$| (F_0(\widehat{Q^n_{u,\delta}}))_j | < \varepsilon. \tag{126}$$

Proof.

Denoting by s, t the functions $[-\pi, \pi] \to \mathbb{C}$ defined by the formulae

$$s(\theta) = \frac{sin((n + \frac{1}{2}) \cdot \theta)}{sin(\frac{\theta}{2})}, \tag{127}$$

$$t(\theta) = e^{u\cdot(cos(\theta)-1)}, \tag{128}$$

we observe that the Fourier series of s, t are given by the formulae (120), (49). Due to (127), (128), we can rewrite (122) in the form

$$| F_0(Q^n_{u,\delta})(\theta) - t(\theta)\cdot s(\theta) | < \varepsilon, \tag{129}$$

from which it immediately follows (due to the convolution theorem) that

$$||(F_0\widehat{(Q^n_{u,\delta})})_j - (\hat{t} * \hat{s})_j|| < \varepsilon. \tag{130}$$

Now, the conclusion of the theorem follows immediately from the combination of Lemma 2.8 with (130), (120), (49).

□

4.3 Proof of Theorem 1.1

In this subsection, we use the analytical machinery developed in the preceding ones to prove Theorem 1.1 of Section 1. Given real numbers ρ, r, ε satisfying the conditions (1), (2), we will define the mapping $\beta^\rho_{r,\varepsilon} : [-\pi, \pi] \to \mathbf{C}$ by the formula

$$\beta^\rho_{r,\varepsilon}(\theta) = Q^n_{u,\delta}(\rho\cdot cos(\theta), \rho\cdot sin(\theta)), \tag{131}$$

with δ defined by (10), ν defined by (3), u defined by (8), and n defined by (13). The following four lemmas show that the function $\beta^\rho_{r,\varepsilon}$ satisfies the conditions of Theorem 1.1, and is very close to the function $b^\rho_{r,\varepsilon}$, defined in Section 1.

The following lemma is obtained from Theorem 4.8 by elementary algebraic manipulation.

Lemma 4.11 *Suppose that under the conditions of Theorem 4.10, the function $\beta^\rho_{r,\varepsilon} : [-\pi, \pi] \to \mathbf{C}$ is defined by (131). Suppose further that either*

$$\rho \in [16\cdot r, \frac{r^2}{4\cdot\delta}], \quad and \quad | \theta | > \frac{8\cdot r}{\rho}, \tag{132}$$

or

$$\rho \in [\frac{r^2}{4\cdot\delta}, \infty], \quad and \quad | \theta | > \frac{8\cdot\sqrt{2}\cdot\delta}{r} + \frac{6\cdot r}{\rho}, \tag{133}$$

or both. Then

$$| \beta^\rho_{r,\varepsilon}(\theta) | < \varepsilon. \tag{134}$$

The following lemma is an immediate consequence of the preceding one.

Lemma 4.12 *Suppose that under the conditions of Theorem 4.10, the function $b^{\rho}_{r,\varepsilon}$ is defined by (131). Then*

$$| b^{\rho}_{r,\varepsilon}(\theta) | < \varepsilon. \tag{135}$$

for all $\theta \in [-\pi, \pi]$, such that

$$| \theta | > \frac{8 \cdot \sqrt{2} \cdot log(\frac{1}{\varepsilon})}{r} + 8 \cdot \frac{r}{\rho}. \tag{136}$$

The following lemma is an immediate consequence of the combination of (59) and Theorem 4.10.

Lemma 4.13 *Suppose that under the conditions of Theorem 4.10, the function $\beta^{\rho}_{r,\varepsilon}$ is defined by (131). Then for all $j \in [-2 \cdot \nu, 2 \cdot \nu]$,*

$$| \widehat{(\beta^{\rho}_{r,\varepsilon})}_j - H_j(\rho) | < \varepsilon. \tag{137}$$

Finally, Lemma 4.14 below is easily obtained from the combination of Lemma 2.13 with (131), (122).

Lemma 4.14 *Suppose that under the conditions of of Theorem 4.10, the functions $\beta^{\rho}_{r,\varepsilon}$, $b^{\rho}_{r,\varepsilon}$, are defined by (131), (15), respectively. Then for all $\theta \in [-\pi, \pi]$,*

$$| \beta^{\rho}_{r,\varepsilon}(\theta) - b^{\rho}_{r,\varepsilon}(\theta) | < \varepsilon. \tag{138}$$

Corollary 4.15 *Obviously, Theorem 1.1 is an immediate consequence of Lemmas 4.12, 4.13, 4.14.*

5 Numerical Considerations and Experiments

5.1 A numerically more attractive procedure

Theorem 1.1 of Section 1 provides a construction of the function $b^{\rho}_{r,\varepsilon}$ satisfying the conditions 1. - 3. of Section 1. However, the function $b^{\rho}_{r,\varepsilon}$ supplied by Theorem 1.1 is in no sense optimal, and in fact has been chosen so as to simplify the proof of Theorem 1.1, not to lead to numerically most efficient schemes. The following construction turns out to provide a function $b^{\rho}_{r,\varepsilon}$ that is considerably more attractive numerically than that provided by Theorem 1.1.

Given real numbers r, ρ, ε such that $0 < r < \rho/4$, and $\varepsilon > 0$, we will define the integer number ν as the smallest real number such that

$$J_j(r) < \varepsilon. \tag{139}$$

for all $j \geq \nu$. We will define the integers m, n by the formulae

$$m = 6 \cdot \nu, \tag{140}$$

$$n = \frac{5}{2} \cdot \nu, \tag{141}$$

and a real number u by the formula

$$e^{-u} \cdot I_{\frac{\nu}{2}}(u) = \varepsilon. \tag{142}$$

Finally, we will define the function $f_{\varepsilon,r} : [-\pi, \pi] \rightarrow \mathbf{C}$, by the formula (14), and the function $b^{\rho}_{r,\varepsilon} : [-\pi, \pi] \rightarrow \mathbf{C}$ by the formula (15).

Observation 5.1 *Obviously, the above procedure defines a function very similar to that provided by Theorem 1.1, as is obvious from Lemmas 2.5, 2.8. However, the analogue of Theorem 1.1 for the construction of this subsection is somewhat subtle; the proof fragments into a large number of cases, depending on the relative sizes of r, ρ, and ε. On the other hand, once the function $b^{\rho}_{r,\varepsilon}$ is obtained, it is quite trivial to verify numerically that it satisfies the conditions 1., 2. of Subsection 1.1, which are the two conditions necessary for $b^{\rho}_{r,\varepsilon}$ to be a translation operator (to a fixed precision ε). Furthermore, our numerical experiments indicate that in most cases, the above construction works better than that provided by Theorem 1.1, in the sense that the coefficients p, q in the formulae (6), (7) are much smaller.*

Observation 5.2 *Clearly, evaluating the function $f_{\varepsilon,r}$ at m equispaced points on the interval $[-\pi, \pi]$ is an order m procedure (see (14)); given $f_{\varepsilon,r}$, the function $b^{\rho}_{r,\varepsilon} : [-\pi, \pi] \rightarrow \mathbf{C}$ (defined in (15)) can be evaluated at m equispaced nodes via the FFT, provided that m is a product of powers of small prime numbers. Thus, in our computations, we altered slightly the definition (140). Specifically, we defined m as the smallest positive integer that is a product of powers of 2, 3, and 5, and is greater than $6 \cdot \nu$. With this modification, the function $b^{\rho}_{r,\varepsilon}$ can be constructed for a cost of the order $m \cdot log(m)$, which is sufficiently fast for most applications.*

5.2 Numerical illustrations

In this subsection, we illustrate the behavior of the functions $\beta^{\rho}_{r,\varepsilon}$ with several figures, as follows.

In Figure 3, we illustrate the behavior of the function G_u with $u = 1000$, by plotting the loci of points x in the plane where $\mid G_u(x) \mid = \varepsilon$, with $\varepsilon = 1.0E-3,\ 1.0E-7,\ 1.0E-12$. The beam-like structure of G_u is quite transparent from this plot.

In Figure 4, we illustrate the behavior of the modulated Gaussian beam $Q^n_{u,\delta}$ by comparing it to the behavior of a Gaussian beam $G_{u,\delta}$ with the same parameters u, δ. Specifically, we plot the loci of points where $\mid Q^n_{u,\delta} \mid = exp(-\delta)$, $\mid G_{u,\delta} \mid = exp(-\delta)$. In the regime we chose for this illustration, both functions behave very much like expanding beams, with the same angle of expansion. The distance between the graphs is roughly equal to n, as it should be (see (113), (114), (118), (119)).

In Figure 5, we illustrate the behavior of the functions $\beta^{\rho}_{r,\varepsilon}$ as ρ grows, for four values of ε ($\varepsilon = 1.0E-3,\ 1.0E-6,\ 1.0E-9,\ 1.0E-12$). Specifically, we plot the size (in radians) Θ of the region around 0 where $\mid \beta^{\rho}_{r,\varepsilon} \mid > \varepsilon$, viewed as a function of ρ. It is quite easy to see that

the region shrinks as ρ grows, apparently converging to some constant, depending on ε. This behavior is in agreement with Lemma 4.12.

In Figure 6, we illustrate the behavior of the functions $\beta^{\rho}_{r,\varepsilon}$ as a tool for the reduction of the computational cost of the Fast Multipole Method. We plot the ratio of the number of nodes required to discretize the function $\beta^{\rho}_{r,\varepsilon}$ at the Nyquist frequency to the number of nodes required to discretize the function ν_n of [6], to the same accuracy and under identical conditions. The ratio is plotted for $\varepsilon = 1.0E-3,\ 1.0E-6,\ 1.0E-9,\ 1.0E-12$, $r = 100$, and $\rho/r \in [4, 40]$. It is easy to see that under these conditions, the improvement is quite dramatic for low-accuracy calculations. When the desired precision is high, the improvement is much less impressive.

Figure 7 is similar to Figure 6, except that here, $r = 500$. Obviously, in this case, the reduction in the computational cost is much greater than for $r = 100$; this is in agreement with Theorem 1.1.

Figure 8 shows the plots of the absolute values of the function $\beta^{\rho}_{r,\varepsilon} : [-\pi, \pi] \rightarrow \mathbf{C}$ with $r = 100$, $\varepsilon = 1.0E-6$, and $\rho = 400,\ 1000,\ 10000$. Here, it is obvious that $\beta^{\rho}_{r,\varepsilon}$ is structured like a bell, with the width of the bell decreasing as ρ increases. By the time $\rho \sim r^2$, the bell shrinks to a point.

Finally, Figure 9 contains a plot of the real part of the function $\beta^{\rho}_{r,\varepsilon} : [-\pi, \pi] \rightarrow \mathbf{C}$. The function is so oscillatory that this plot is not very informative. However, it is clear from Figures 8, 9 that while the *absolute value* of $\beta^{\rho}_{r,\varepsilon}$ looks very much like a bell, the function $\beta^{\rho}_{r,\varepsilon}$ itself is quite oscillatory, except near $\theta = 0$.

6 Generalizations and Applications

Obviously, the purpose of this paper is purely technical - to construct numerical tools to be used in the design of Fast Multipole Methods for the Helmholtz equation. Furthermore, in a vast majority of applications, the problems are three-dimensional, so that the principal (though by no means the sole) purpose of a two-dimensional scheme is to serve as a model before three-dimensional algorithms are attempted.

The construction of this paper is trivially generalized to arbitrary real Helmholtz coefficients by rescaling. The construction extends to complex Helmholtz coefficients easily, as long as the real part of the Helmholtz coefficient is positive; in this case, the proofs have to be modified slightly. The construction becomes numerically unstable for Helmholtz coefficients with large negative imaginary parts.

Our numerical experiments show that the construction of the preceding section can be sharpened somewhat, especially for relatively small r and ρ. In other words, there exist versions of the function $\beta^{\rho}_{r,\varepsilon}$ that have the same frequency content as those constructed in the preceding section, and that are small on a greater part of the interval $[-\pi, \pi]$. However, in our experiments we used optimization techniques to construct such functions, at a significant cost in CPU time (the cost of our procedure is of the order $O(m^3)$, with a fairly large constant). At the present time, the possibility of more efficient schemes of this type is under investigation.

Extension of the results of this paper to three dimensions is quite straightforward, and a paper reporting it is in preparation. The author is currently in the process of incorporating the construction of Section 5 of this paper into a Fast Multipole scheme for the solution of two-dimensional scattering problems. These results, and their extension to three dimensions, will be reported at a later date.

7 Acknowledgments

The author would like to thank Professor R.R. Coifman for many useful discussions, and for his continuing interest and support. He is indebted to Dr. Matviyenko and Dr. Wandzura for their help. Special thanks are due Professor W.C. Chew, Dr. R.L. Wagner, and Dr. J.M. Song for providing a most stimulating competition.

References

[1] M. Abramovitz and I. Stegun, *Handbook of Mathematical Functions*, Applied Math. Series (National Bureau of Standards), Washington, DC, 1964.

[2] R. L. Wagner, W. C. Chew, *A Ray-Propagation Fast Multipole Algorithm*, Microwave and Optical Technology Letters, Vol. 7, No. 10, July 1994.

[3] J.M. Song, W. C. Chew, *Fast Multipole Solution using Parametric Geometry*, Microwave and Optical Technology Letters, Vol. 7, No. 16, November 1994.

[4] R. Coifman, V. Rokhlin, S. Wandzura, *Faster Single-Stage Multipole Method for the Wave Equation*, 10-th Annual Review of Progress in Applied Computational Electromagnetics, Vol. 1, pp. 19-24, Monterey, CA, March, 1994, Applied Computational Electromagnetics Society.

[5] N.S. Koshliakov, M.M. Smirnov, and E.B. Gliner, *Differential Equations of Mathematical Physics*, North-Holland, Amsterdam, 1964.

[6] V. Rokhlin, *Rapid Solution of Integral Equations of Scattering Theory in Two Dimensions*, Journal of Computational Physics, 86(2) : 414 (1990).

[7] V. Rokhlin, *Diagonal Forms of Translation Operators for the Helmholtz Equation in Three Dimensions*, Applied and Computational Harmonic Analysis, v. 1, 1993, pp. 82-93.

[8] G.N. Watson, *A Treatise on the Theory of Bessel Functions*, Cambridge University Press, Cambridge, 1980.

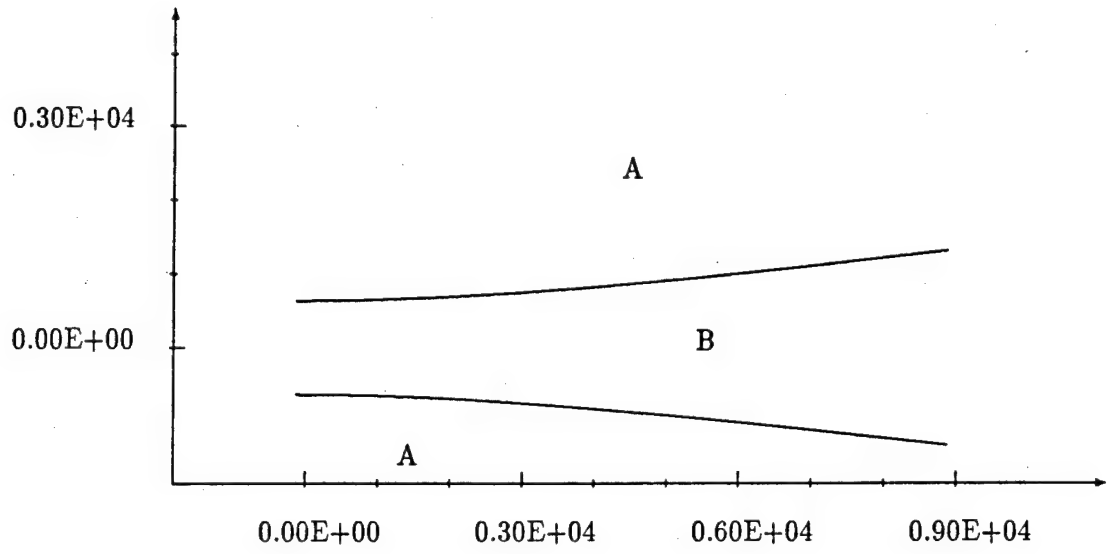

Figure 1: Regions A, B, with $u = 10000$, $\delta = 40$

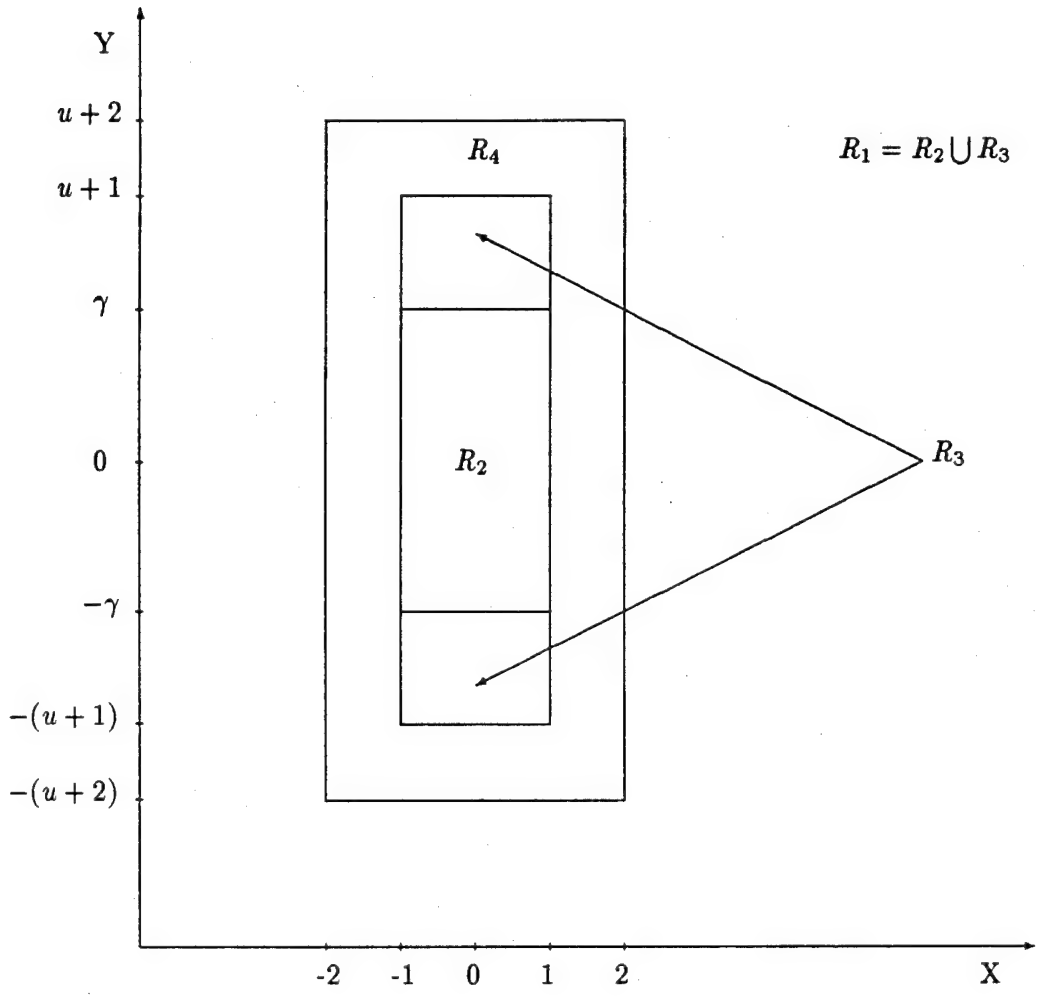

Figure 2: Rectangles R_1, R_2, R_3, R_4; drawn not to scale

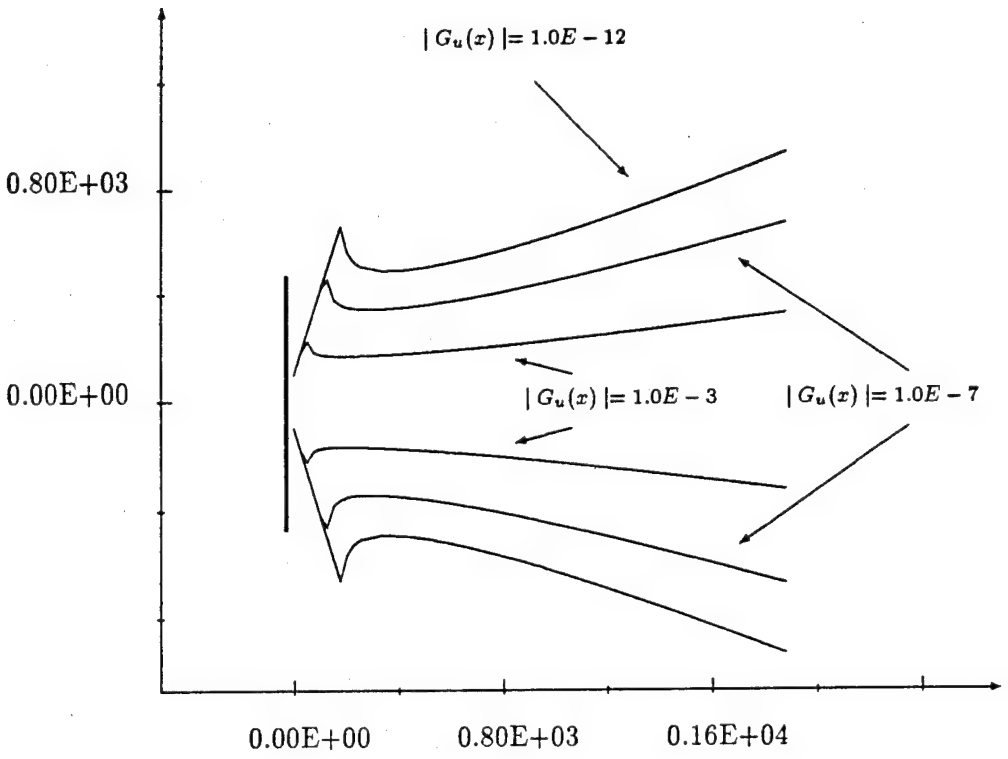

Figure 3: Gaussian beam G_u, with $u = 1000$; drawn to scale.

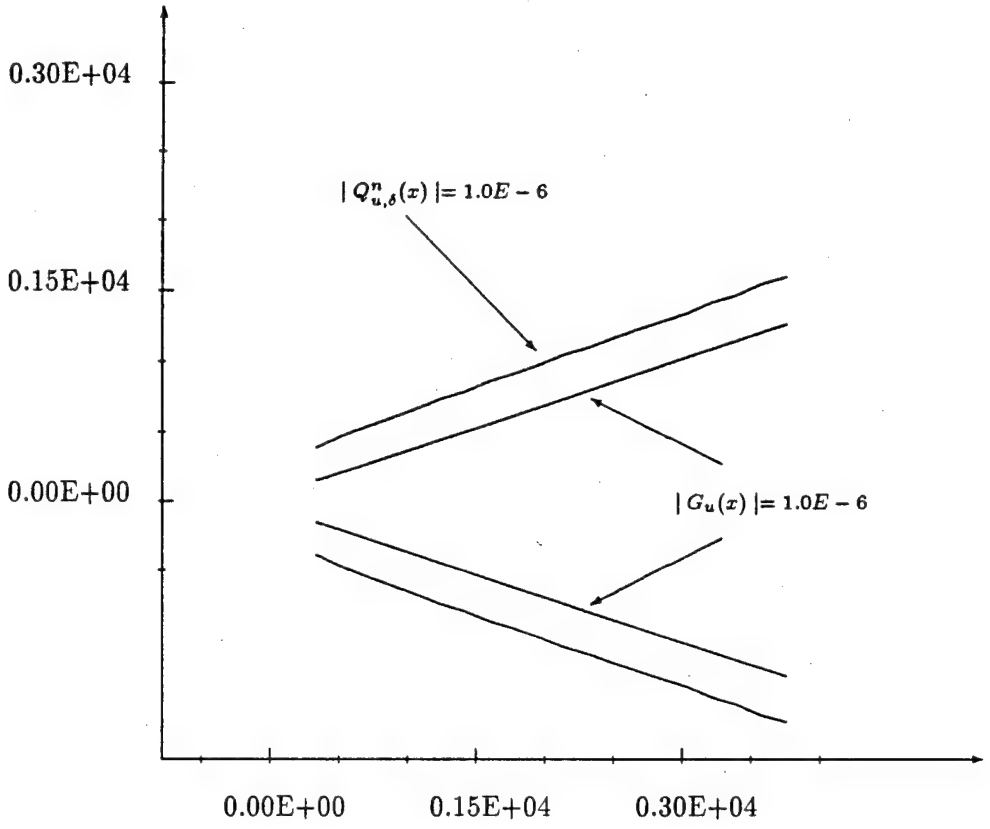

Figure 4: Functions $Q^n_{u,\delta}$, $G_{u.\delta}$, with $u = 168$, $n = 311$, $\delta = 13.82 \approx -log(1.0E-6)$

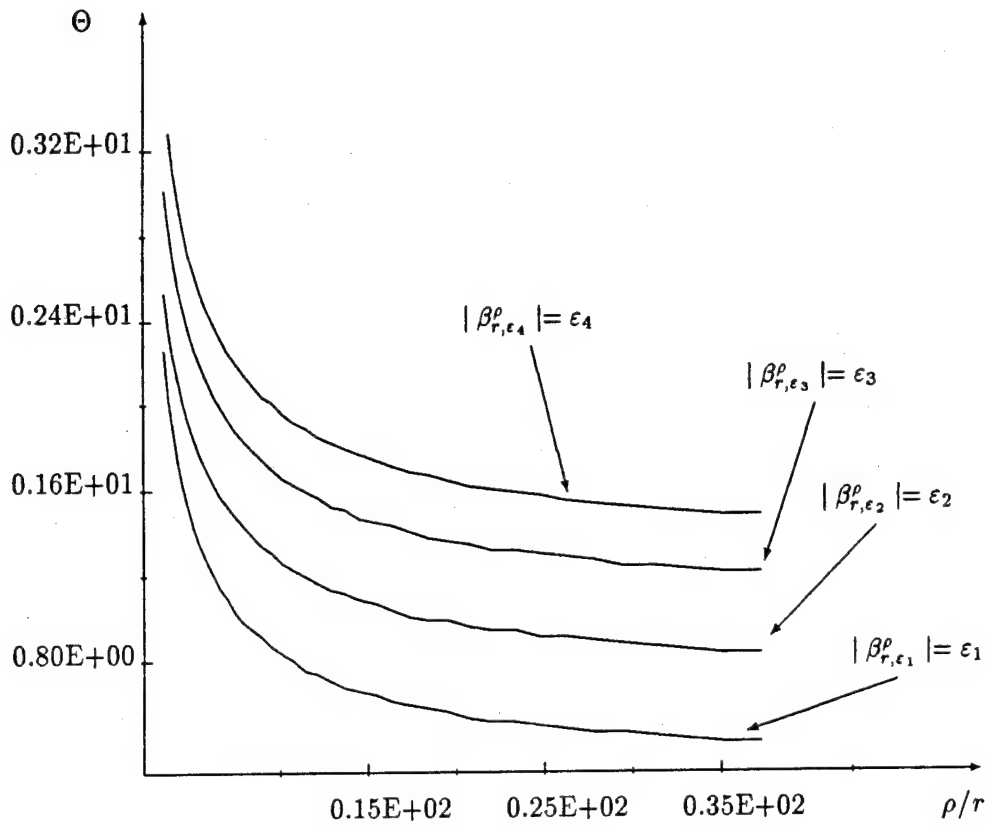

Figure 5: Functions $\beta^{\rho}_{r,\varepsilon}$, with $r = 100$, $\varepsilon_1 = 1.0E-3$, $\varepsilon_2 = 1.0E-6$, $\varepsilon_3 = 1.0E-9$, $\varepsilon_4 = 1.0E-12$.

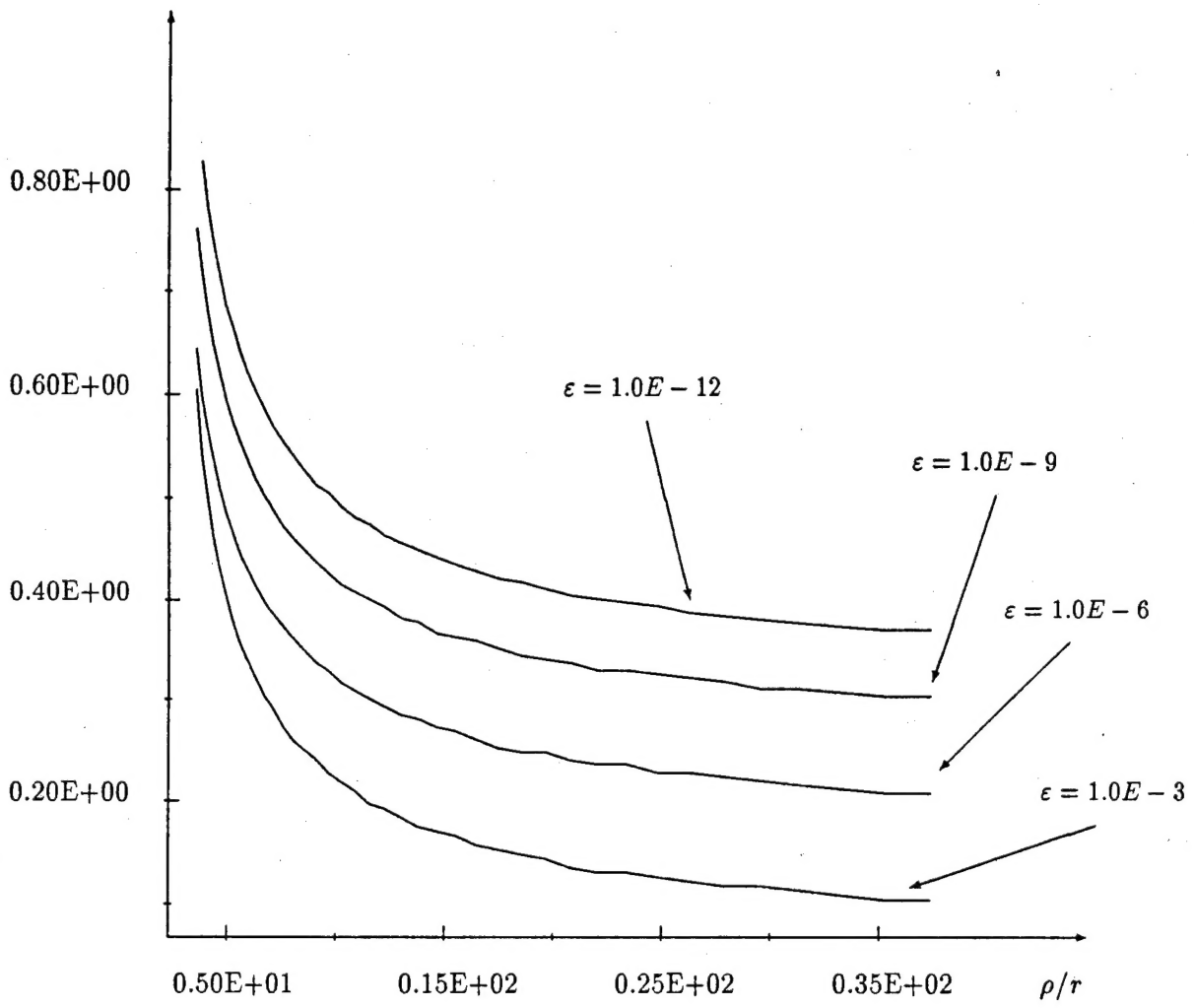

Figure 6: Improvement in the number of nodes in the discretizations of functions $\beta^{\rho}_{r,\varepsilon}$, as a function of ρ/r; with $r = 100$, and $\varepsilon_1 = 1.0E-3,\ 1.0E-6,\ 1.0E-9,\ 1.0E-12$.

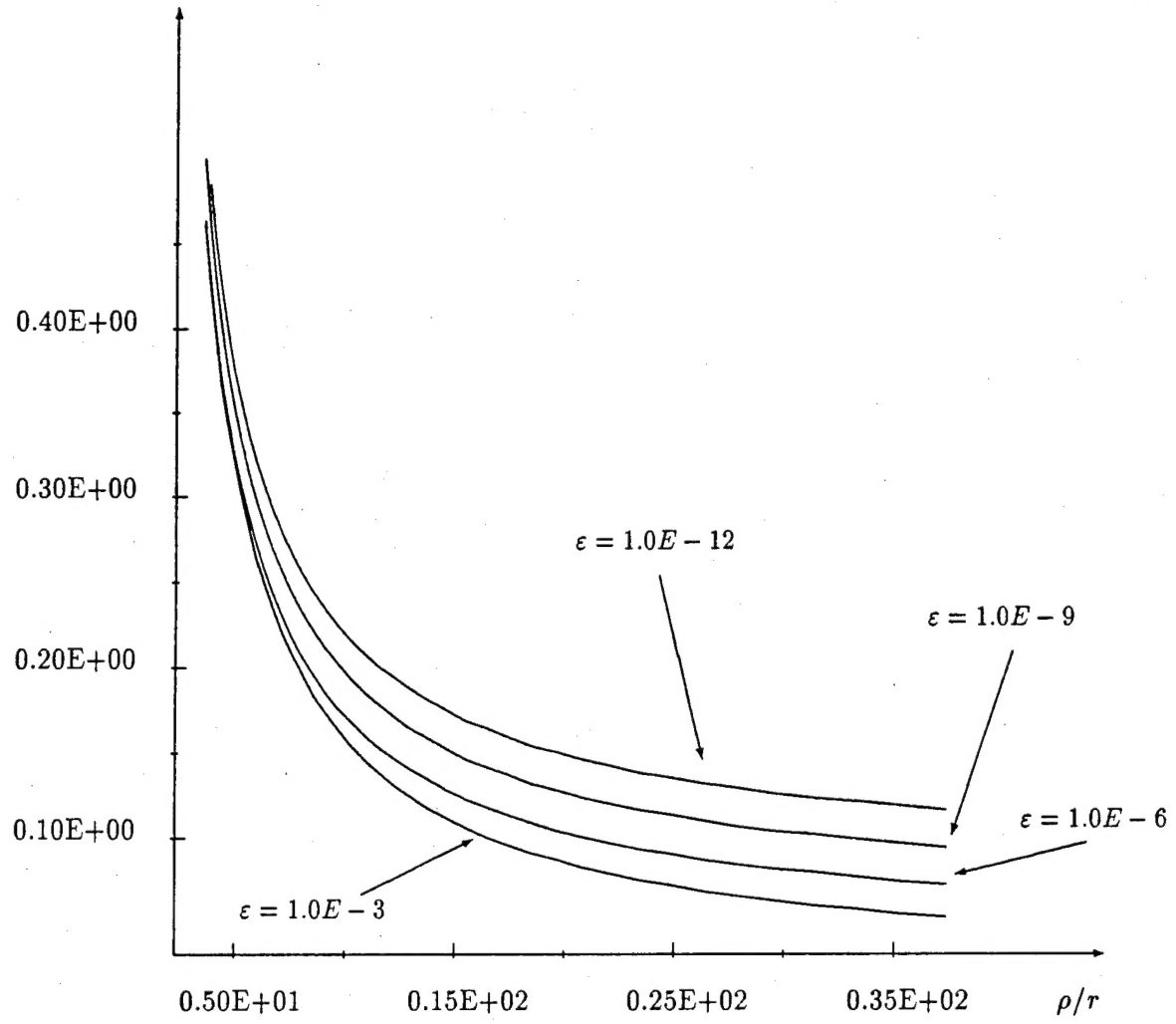

Figure 7: Improvement in the number of nodes in the discretizations of functions $\beta^{\rho}_{r,\varepsilon}$, as a function of ρ/r; with $r = 500$, and $\varepsilon_1 = 1.0E-3,\ 1.0E-6,\ 1.0E-9,\ 1.0E-12$

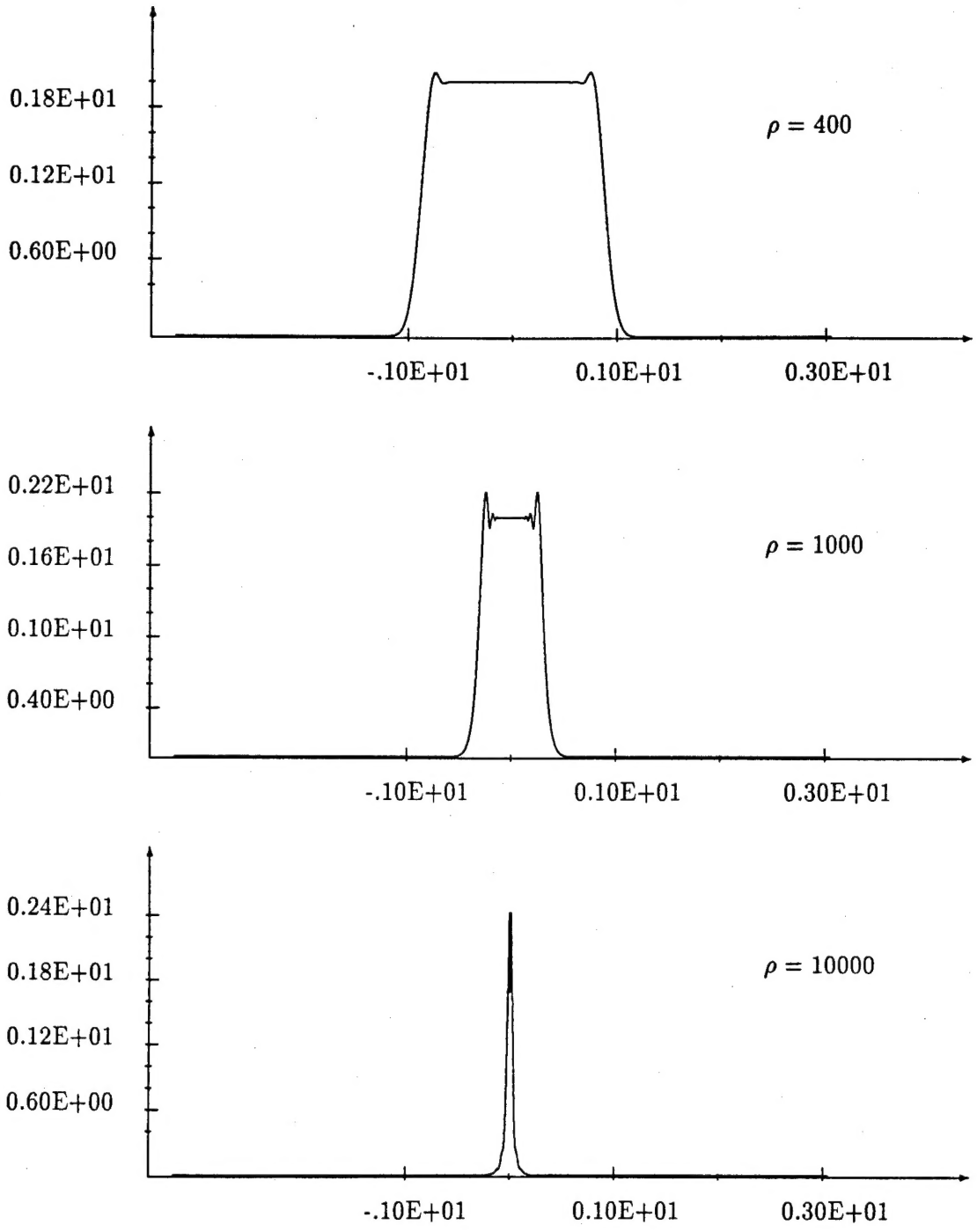

Figure 8: Absolute values of the function $\beta^{\rho}_{r,\varepsilon}$, with $r = 100$, $\varepsilon = 1.0E-6$, and $\rho = 400,\ 1000,\ 10000$

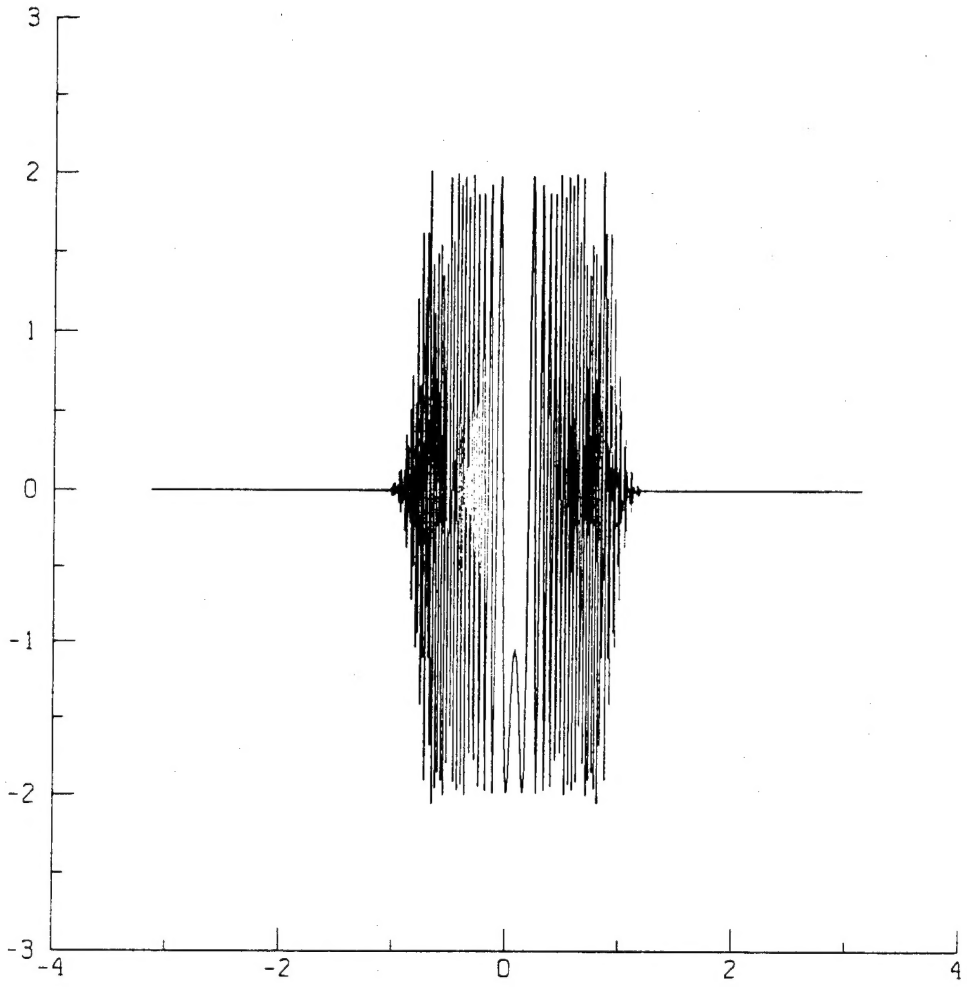

Figure 9: Real part of the function $\beta^{\rho}_{r,\varepsilon}$, with $r = 100$, $\varepsilon = 1.0E-6$, and $\rho = 400$